

Published in final edited form as:

Heart Rhythm. 2008 November ; 5(11): 1587–1596. doi:10.1016/j.hrthm.2008.08.030.

Electrophysiological mechanisms of antiarrhythmic protection during hypothermia in winter hibernating versus nonhibernating mammals

Vadim V. Fedorov, PhD^{*,†}, Alexey V. Glukhov, PhD^{*,†}, Sangita Sudharshan, BS^{*}, Yuri Egorov, MS[†], Leonid V. Rosenshtraukh, PhD[†], and Igor R. Efimov, PhD^{*}

^{*}Department of Biomedical Engineering, Washington University, St. Louis, Missouri

[†]Cardiology Research Center, Moscow, Russia

Abstract

BACKGROUND—Robust cell-to-cell coupling is critically important in the safety of cardiac conduction and protection against ventricular fibrillation (VF). Hibernating mammals have evolved naturally protective mechanisms against VF induced by hypothermia and reperfusion injury.

OBJECTIVE—We hypothesized that this protection strategy involves a dynamic maintenance of conduction and repolarization patterns through the improvement of gap junction functions.

METHODS—We optically mapped the hearts of summer-active (SA) and winter-hibernating (WH) ground squirrels *Spermophilus undulatus* from Siberia and nonhibernating rabbits during different temperatures (+3°C to +37°C).

RESULTS—Midhypothermia (+17°C) resulted in nonuniform conduction slowing, increased dispersion of repolarization, shortened wavelength, and consequently enhanced VF induction in SA ground squirrels and rabbits. In contrast, wavelength was increased during hypothermia in WH hearts in which VF was not inducible at any temperature. In SA and rabbit hearts, but not in WH, conduction anisotropy was significantly increased by pacing acceleration, thus promoting VF induction during hypothermia. WH hearts maintained the same rate-independent anisotropic propagation pattern even at 3°C. connexin 43 (Cx43) had more homogenous transmural distribution in WH ventricles as compared to SA. Moreover, Cx43 and N-cadherins (N-cad) densities as well as the percentage of their colocalization were significantly higher in WH compared to SA epicardium.

CONCLUSION—Rate-independent conduction anisotropy ratio, low dispersion of repolarization, and long wavelength—these are the main electrophysiological mechanisms of antiarrhythmic protection in hibernating mammalian species during hypothermia. This strategy includes the improved gap junction function, which is due to overexpression and enhanced colocalization of Cx43 and N-cad.

Keywords

Hibernation; Ventricular fibrillation; Conduction anisotropy; Optical mapping; Hypothermia

© 2008 Heart Rhythm Society. All rights reserved.

Address reprint requests and correspondence: Dr. Vadim V. Fedorov, Department of Biomedical Engineering, Washington University, Campus Box 1097, One Brookings Drive, St. Louis, Missouri 63130-4899. E-mail address: vadimfed@gmail.com.. Drs. Fedorov and Glukhov contributed equally to this work.

Introduction

Hibernating mammals represent a unique model that is characterized by the puzzling ability to undergo rapid (100-fold) changes in metabolic rate, protein expression, oxygen consumption, and heart rate.¹⁻³ During the winter season, the hibernators undergo bouts of torpor (winter hibernating state [WH]) lasting approximately 7 to 14 days, with periods of interbout arousal approximately 1 day. In torpor, the core body temperature can drop as low as -2.9°C .⁴ Unlike human and other nonhibernating mammals, hibernators do not experience life-threatening cardiac arrhythmias, reperfusion injuries, or other ill effects during either the onset of hibernation, a relatively slow process involving drastic changes in levels of protein expression, or during arousal, which takes 1 to 3 hours and results in an increase in protein expression.^{1,2,5} Recently, we have shown that in contrast to nonhibernators, the WH ground squirrel (GS) *Spermophilus undulatus* has a slow but safe ventricular activation at extreme hypothermia ($+3^{\circ}\text{C}$), possibly caused by upregulation of connexin 43 (Cx43) and Cx45.^{5,6} Moreover, we observed seasonal differences in conduction safety: WH hearts had high conduction velocity and low stimulation threshold as compared to summer-active (SA) hearts at all temperatures.

The goal of the study was to investigate the electrophysiologic mechanisms through which improved cell-to-cell coupling contributes to the resistance of hypothermia-induced ventricular tachyarrhythmias. To test this hypothesis, we investigated the role of hypothermia-induced electrophysiological heterogeneities of conduction and repolarization as well as the wavelength of reentry in the onset of ventricular fibrillation (VF) in WH and SA Siberian GS. The study investigated dynamic changes of conduction anisotropy during different temperatures. We further aimed to study another important player in the formation of gap junctions, the adherens junctional protein N-cadherin (N-cad),⁷ and to determine the contribution of both Cx43 and N-cad to enhanced cell-cell coupling.

Methods

Animals

All procedures were approved by Washington University in St. Louis and the Cardiology Research Center (Moscow) Animal Care and Use Committees.

We studied the wild hibernating GS *Spermophilus undulatus*. Animals were captured in August 2004 and 2005 in the coldest region of Siberia, which is located in the Lena river valley near the city of Yakutsk, Russia.⁵ We used animals in 2 different states, which are known to have significant differences in metabolism and physiology: SA ($n = 12$, 556 ± 61 g) and WH ($n = 14$, 612 ± 46 g). We also used 8 rabbits (Russian breed Shinshilla) as a nonhibernating control.

Optical mapping experiments

The optical mapping system and Langendorff-perfused GS and rabbit heart have been previously described.⁵ The entire anterior ventricular epicardial surface was mapped with a 127×128 -pixel charge coupled device (CCD) camera (Dalsa, Waterloo, Canada) with a field-of-view of approximately 16×16 mm to 18×18 mm. The excitation—contraction uncoupler 2,3-butanedione monoxime (BDM) (15 mmol/l; Fisher Scientific, Fair Lawn, New Jersey) was added to the perfusate to suppress motion artifacts.

The pacing site was located on the anterior left ventricular (LV) epicardium midway between apex and base. The pacing current was at least 4X the pacing threshold. We used the restitution S1-S1 protocol as described earlier.⁸ Hearts were paced with a basic cycle length from 400 to 200 ms (at 37°C), from 1,000 to 300 ms (at 27°C), and from 2,000 to 500 (at 17°C) in steps of 50 ms, and further in steps of 10 ms until 1:1 capture failed or ventricular tachycardias,

including VF, occurred. Arrhythmias that continued for more than 1 minute were electrically defibrillated by a custom-made LV implantable defibrillation lead and defibrillator (Gold SM 1211). The shortest pacing S1 interval to capture without Wenckebach periodicity was deemed the ventricular functional refractory period (VFRP).

A custom Matlab (Math Works, Inc. Novi, MI) computer program was used to analyze the optical action potentials (AP) in the ventricles as previously described.⁹ First, we filtered the signal using the low-pass Butterworth algorithm at 200 Hz. Then, the 2 control beats of the optical signal were averaged and normalized between -85 and 15 mV. Finally, AP duration at 90% of repolarization levels (APD₉₀) and maximum upstroke derivative (dV/dt_{\max}) were calculated for each AP using the normalized optical signal and its derivatives (Figure 1B). Control dV/dt_{\max} values for all tissues were from 6 V/s to 14 V/s. These values are significantly lower than the dV/dt_{\max} of AP recorded by microelectrodes because of the averaging of optical signals from different cell layers and filtering.⁹

To characterize a spatiotemporal pattern of repolarization, the following parameters were measured or calculated in all the animals groups at different temperatures: APD₉₀ for 256 epicardial sites, standard deviation of mean APD₉₀ (SD-APD₉₀, in ms), and maximum dispersion (D_{\max} , in ms). D_{\max} was calculated as the difference between the minimum and the maximum values of APD₉₀ along the field of mapping.⁸

Immunohistochemistry

After the blood was washed from the hearts with Tyrode solution for 10 to 15 min (SA n = 4, WH, n = 4), hearts were embedded in Tissue-Tek OCT, (Torrance, CA) compound, frozen, and cryosectioned parallel or perpendicular to the epicardium. Sections were then stained for fluorescence immunohistochemistry with commercially available antibodies: rabbit Cx43 (Sigma, St. Louis, Missouri; 1:1000 dilution) + mouse α -actinin (Sigma, 1:1600), rabbit α -actinin, mouse N-cad (Sigma, 1:100), or rabbit Cx43 + mouse N-cad. Primary stains were applied overnight, and then secondary antibodies were applied for 2.5 hours. Confocal imaging was performed using a 40X lens on a Nikon C1/80i confocal microscope (Melville, NY). Protein density was measured using a custom Matlab program as previously described.¹⁰

The epicardium was defined as tissue within 100 μm from the outer surface of the heart, the endocardium as tissue within 100 μm from the inner surface, and the midmyocardium as the remaining tissue not within 100 μm of either surface.

Colocalization analysis

Colocalization plots were used to determine the amount of Cx43 that colocalized with N-cad. In a 2-channel confocal image, each voxel has 2 intensity values (ranging from 0 to 4,095 in a 12-bit image), 1 for each red and green staining. Voxels with intensities <1,024 were considered background fluorescence and were excluded from analysis. A colocalization plot, generated with Volocity (Improvision, Inc., Lexington, Massachusetts), displays these intensity values as a function of each other. By definition, 2 proteins are highly colocalized in a particular volume when fluorescence intensities corresponding to these 2 proteins are high in the voxel corresponding to this volume.¹¹ Therefore, if 2 proteins are colocalized in many voxels, the colocalization plot will contain a significant diagonal distribution. Voxels with the highest degree of colocalization will be displayed in the upper-right quadrant. In contrast, if the 2 proteins are not colocalized, the colocalization plot shows voxel values near each axis, with no diagonal elements present. We consider colocalized Cx43 signal as functional Cx43. Total Cx43 was defined as the number of voxels above the threshold 1,024, and functional Cx43 as voxels above 1,024 in both red and green.

Statistical analysis

Group data were represented as mean \pm standard error. Comparisons between groups of data were performed using an unpaired *t* test, chi-squared analysis with Yates correction, and Kolmogorov-Smirnov test. A value of $P < .05$ was considered statistically significant.

Results

Activation pattern of ventricles under control and hypothermia conditions

Decreasing temperature from $+37^{\circ}\text{C}$ to $+3^{\circ}\text{C}$ did not induce cardiac arrest in any SA ($n = 7$) or WH ($n = 7$) hearts, as we previously reported.⁵ In contrast, the rabbit heart ($n = 6$) experienced a complete loss of excitability at $12^{\circ}\text{C} \pm 1^{\circ}\text{C}$. In all animals, the temperature reduction resulted in an increased pacing threshold. Table 1 summarizes the excitation threshold data in rabbit and GS LV. A significant increase in the pacing threshold was observed in both rabbit and SA ventricles at temperatures as low as 27°C . In contrast, the increase in pacing threshold for WH became significant only after a reduction of temperature to $+7^{\circ}\text{C}$. Moreover, the pacing threshold in WH was significantly lower compared to SA and rabbit ventricles at all temperatures.

Hypothermia induced during the basic pacing cycle length caused a significant increase of optical action potential duration (APD) as well as its dispersions and in rabbit and SA hearts compared to WH. At all temperatures, WH hearts had shorter APD (Table 1). However, the VFRP was increased significantly more in WH than SA (Table 2). This result shows the existence of postrepolarization refractoriness in WH but not in SA hearts.

The temperature reduction leads to significant decreases in longitudinal and transversal conduction velocities (CV_L and CV_T) in rabbit compared to GS hearts. Moreover, hypothermia induced an increase of conduction anisotropy (CV_L/CV_T) in SA and rabbit heart, but not in WH ventricles because of more significant CV_T slowing in these hearts (Tables 1 and 2).

Figure 1A shows representative activation maps of optical signals from the LV epicardium of WH GS and rabbit heart. Figure 1B shows superimposed upstrokes and their first derivative dV/dt of representative action potentials recorded from adjacent sites along the fast and slow axis of impulse propagation. Although conduction slowed, the Langendorff-perfused WH hearts almost maintained the same pattern of epicardial activation during basic pacing at all studied temperatures down to 3°C . In contrast to WH, rabbit hearts during hypothermia resulted in a significant increase of conduction anisotropy because of a depression of transversal CT along the transverse direction up to the block as evidenced by the crowding of isochronal lines (Figure 1B) and the greater delay between action potential upstrokes (Figure 1A and B, rabbit).

The excitation wave was almost blocked in the transverse direction of propagation (anisotropy index was >4) at 12°C . The base of the LV was activated by a wide front of excitation in a retrograde and/or intramural conduction as a result of the wave front diving below the hypothermia-induced epicardial conduction block and resurfacing into epicardial tissue.⁹

Figure 2A shows a dependence in conduction anisotropy of pacing cycle length in WH, SA, and rabbit hearts at different temperatures. Conduction anisotropy in WH was lower as compared with SA and rabbit ventricles during hypothermia and at all pacing cycle lengths (Figure 2A, Tables 1 and 2). Even at 37°C , conduction anisotropy in rabbit hearts significantly increased at shortened pacing cycle lengths, which were performed during VFRP measurements. Rabbit hearts had a steeper slope of anisotropy restitution, which is a cycle length dependence in anisotropy. Hypothermia resulted in a significant increase in anisotropy at a basic cycle length and made the slope of anisotropy curve steeper in rabbit hearts and SA, but not in WH hearts. Maximums from conduction anisotropy values were 3.4 ± 0.1 in rabbit,

2.7 ± 0.1 in SA, and only 2.1 ± 0.1 in WH hearts. These values were achieved at 17°C during the fastest cycle length (VFRP) (Table 2).

Figure 2B shows the temperature dependence of the main ventricular electrophysiological parameters: VFRP, minimal CV_L , and CV_T , which were measured during VFRP, and wavelength for reentry ($\text{WL} = \text{VFRP} \times \text{minCV}_T$).¹² The WL values were not different between animal groups at 37°C . The WL increased in WH during hypothermia. In contrast, we observed a significant reduction of WL in rabbits and SA during hypothermia.

Both wavelength shortening and increased conduction anisotropy enhanced the vulnerability to ventricular arrhythmias in rabbit and SA hearts during hypothermia (Figure 2C). Hypothermia increased the probability of pacing-induced VF in rabbit and SA hearts from 17% to 67% ($P < .01$) and 0% to 17%, respectively. In contrast, we could not induce VF in WH hearts at any temperature.

Figure 3 shows an example of VF occurrence in the rabbit heart during fast pacing at 17°C . The gradual shortening of the pacing interval from 2,000 ms to 470 ms leads to a slowing of conduction velocities and increases of anisotropy. A further increase in stimulation frequency resulted in the occurrence of conduction blocks in the transverse direction and induction reentrant wave breaks, which induced a loss of pacing capture (see electrogram recording in Figure 3). Thus, this mechanism of VF induction includes several seconds of interference pacing with reentrant arrhythmias. After stop pacing we observed a figure-eight type of reentry resulting in sustained VF (V1 and V2 maps in Figure 3).

Seasonal expression of Cx43 and N-cadherin

Alterations in either the total amount or the distribution of the gap junction protein Cx43 has been shown to promote conduction abnormalities and facilitate arrhythmias.^{13,14} Therefore, we tested the hypothesis that the transmural distribution of Cx43 may be altered in GS during summer and winter. Epicardial Cx43 density in SA hearts was found to be significantly decreased as compared with the epicardial density for WH hearts. Transmural expression of Cx43 was significantly altered in SA hearts as compared with WH hearts (Figure 4). The WH hearts did not show significant changes in Cx43 density from epicardium to endocardium. However, in SA, midmyocardial Cx43 density was significantly higher compared with the epicardium.

Epicardial parallel section double staining of Cx43 and N-cad showed a significant increase in the density of both proteins in WH compared to SA hearts (Figure 5A). We found that there was a greater Cx43 and N-cad colocalization in WH ($50\% \pm 3\%$) compared to SA ($39\% \pm 2\%$, $P < .05$ vs. WH). On average, the total amount of Cx43 signal that was colocalized with N-cadherin increased by 1.7-fold in the epicardial layers of WH hearts relative to SA ($P < .01$) (Figure 5B).

Discussion

Electrophysiological mechanisms of arrhythmia protection in hibernator heart

It is well established that predisposition to onset of life-threatening arrhythmias such as ventricular tachycardia (VT) and VF are frequently associated with the following electrophysiological factors: dispersion of repolarization/refractoriness, slow conduction, high anisotropy of conduction, and short wavelength for reentry.^{15,16} Dynamic change in action potential duration and conduction within the framework of the restitution theory can explain tissue predisposition to wave break and induction of reentry.^{17,18} However, analysis of rate-dependent changes has not been applied to conduction anisotropy in the settings of reentry induction.

Hibernating species present a particularly intriguing model of antiarrhythmia protection, being resistant to VF in contrast to most mammals.¹ During hypothermia, ventricular arrhythmias are the most common cause of death in humans.¹⁹ Hypothermia can induce the downregulation of Cx43 expression and/or dephosphorylation, and thus produces cell-to-cell uncoupling as evidenced by reduced conduction velocity^{5,20,21} and increased heterogeneity of conduction, and repolarization.²² These effects form the substrates for induction and maintenance of VF. In contrast, hibernating mammalian species do not experience cardiac dysfunction and/or malignant arrhythmias during either the onset of hibernation or arousal, during which core body temperature can be changed more than 30°C during 1 to 3 hours.⁴

Saitongdee et al²³ proposed that Cx43 overexpression in hamsters during the winter could be a mechanism of protection against conduction block and arrhythmia during hibernation and arousal. We confirmed this hypothesis by optical mapping of WH and SA Siberian GS hearts. This species is one of the most resilient mammalian hibernators, able to adapt to and spontaneously arouse from core body temperatures as low as -2°C without freezing.^{4,24} We found that they maintained spontaneous sinus rhythm, safe propagation through the entire conduction system, and normal pattern of ventricular excitation even at 3°C temperatures.^{5,6,25} However, all rabbit and rat hearts lost excitability at 12°C ± 1°C and 10°C ± 1°C, respectively. At any temperature, WH ventricles had faster longitudinal conduction velocity and lower excitation threshold compared to SA. Immunolabeling showed that Cx43 and Cx45 were significantly upregulated in WH as compared to SA myocardium.⁵

In this study, we investigated for the first time the electrophysiological and molecular mechanisms of arrhythmia resistance during hibernation in detail. We found significant slowing of CV_T than CV_L during the acceleration of pacing in rabbits and SA. Hypothermia significantly increased the slope of conduction anisotropy restitution and thus provoked induction of reentrant arrhythmias (Figures 1 to 3). Progressive cycle length shortening resulted in slower conduction and increased anisotropy, which formed a functional substrate^{26,27} for arrhythmia occurrence in rabbit and SA hearts, but never in WH (Figures 1 to 3). The WH hearts maintained both wavelength and anisotropic ratio at all temperatures (down to 3°C). We believe that these electrophysiological features of WH myocardium can explain why VF was not inducible at any temperature in these hearts.

Progressive hypothermia caused a greater increase in refractory period per increase in APD in WH than SA. This effect resulted in the development of postrepolarization refractoriness during hibernation (Table 1). Hibernation-induced postrepolarization refractoriness may prevent the slowing of conduction during premature beats and tachyarrhythmia induction.^{28,29} Thus, the development of postrepolarization refractoriness during hibernation may be an additional protective mechanism against arrhythmia associated with hypothermia and reperfusion. Moreover, the increase in VFRP almost compensated for conduction slowing during hypothermia and thus prevented proarrhythmic decrease of wavelength in WH hearts.

Role of gap junction in the hibernator antiarrhythmia protection

Numerous studies have shown that abnormal intercellular coupling through the main cardiac gap junction proteins Cx43, Cx40, and Cx45 is an important mechanism for atrial and ventricular heterogeneities of repolarization and propagation.³⁰⁻³³ Abnormal function of Cx43 could be responsible for life-threatening ventricular arrhythmias, including VT/VF.^{34,35} However, hypothermia can also induce gap junction channel uncoupling through the reduction of conductance of Cx43 channels.³⁶ It was shown that pharmacological gap junction uncoupling may enhance intrinsic nonuniformities in conduction.^{33,37} Recent studies have shown that the loss of Cx43 in knockout mice^{34,35} is directly correlated with anisotropic slowing of conduction, thus an increased propensity for arrhythmogenesis. In contrast, pharmacological preservation of intercellular coupling diminished conduction slowing and

heterogeneous repolarization, eliminating arrhythmogenic substrates.³⁸ A gap junction opener was proposed to treat ventricular tachycardia during ischemia by opening of Cx43.^{38,39} Alternatively, gap junction upregulation is proposed here to improve conduction safety and thus to protect myocardium against life-threatening tachyarrhythmia.

Cardiac N-cad is an integral part of the intercalated disc junction, essential for the adherens junctions in myocyte, Cx43 delivery to cell—cell contact, and thus the establishment of Cx43.^{40,41} Conditional deletion of this important adherens junctional protein (N-cad) in the adult mouse heart leads to a complete dissolution of the intercalated disc structure and a significant decrease in the Cx43 expression. This deletion results in dilated cardiomyopathy, conduction slowing, and higher conduction anisotropy and thus spontaneous ventricular tachycardia and arrhythmic death.⁷ In contrast, mice with cardiac overexpression of N-cad suffer from cardiac hypertrophy and further structural abnormalities.⁴²

The intracellular co-assembly of connexin and cadherin is required for gap junction and adherens junction formation, a process that likely underlies the intimate association between gap junction and adherens junction formation.⁴³ Moreover, N-cad—mediated adhesion is critical for maintaining Cx43 at the plasma membrane thus for cardiac conduction.^{41,43,44}

We found that both gap junction proteins Cx43 and N-cad were overexpressed during hibernation season (Figure 5). Akar et al¹⁴ proposed that Cx43 is functional only when it is expressed alongside N-cad. We observed a significant increase in the colocalization of these proteins in WH. Based on this theory, our results suggest that there is a greater functional Cx43 in WH than SA (Figure 5). This observation indicates that there may be stronger adherence between myocytes during the hibernation period, resulting in stronger connections and synchronized contractions.

The remodeling process of gap junctions during hibernation is completely different from the remodeling in knockout Cx43 mice³⁵ as well as in aged mice,⁴⁵ in which heterogeneous downregulation of Cx43 takes place. The hibernator's strategy during the winter is to improve the function of normal gap junctions. This conclusion confirms that even during the summer these animals have more resistance to arrhythmia compared to nonhibernating rabbits and rats.

It was shown that heterogeneity of gap junction proteins between epicardium and midmyocardium can lead to anisotropic conduction and reentrant ventricular arrhythmias.³² If hypothermia is induced, these changes may become more apparent and more aggravated. In WH we found more homogeneous, transmural Cx43 expression (Figure 4), which may aid in preventing any differences in the transmural distribution of action potential duration and conduction safety.

Previously, we found that another cardiac gap junction protein Cx45 also overexpressed in the Siberian GS ventricle during hibernation.⁵ The Cx45 signal was clearly observed in the intercalated disk area in the LV endocardium of the WH heart. For all animals in the SA and winter active groups, no Cx45 signal was observed. The quantitative comparison was impossible for Cx45 immunolabeling because of a lack of signal in the SA myocardium and low Cx45 signal in epicardium of WH. However, we still believe that Cx45 could be another potential contributor to the arrhythmia protective effects in WH.

We emphasize that not only Cx43 with N-cad is colocalized highest in the WH, but also there is more total Cx43. The CV was affected by hypothermia in both directions in all animals. However, in WH transversal CV slowing was less than SA. Thus, probably because of higher total and colocalized Cx43, WH hearts can almost keep the same anisotropy ratio during different temperatures. We found statistical differences between SA and WH anisotropies only

during hypothermia and relatively fast pacing—extreme condition which affected the conduction safety factor.

Ionic mechanism of hibernator resistance to hypothermia-induced cardiac arrest

Although it is likely that Cx43 and N-cad play an important role, many other mechanisms such as ionic channels remodeling may be involved in arrhythmia protection of hibernator hearts. It has been proposed that the both Ca^{2+} and Na^{+} currents may be responsible for the excitation of the hibernator myocytes at about 5°C .^{46,47} Unfortunately, only a few studies were performed to investigate this important issue. Liu et al⁴⁷ showed that in hedgehog cardiac preparations, the peak of Ca^{2+} current did not significantly change at low temperatures, and the Na^{+} current was less suppressed by the cooling in hibernator than in rats. Another study by Yatani et al⁴⁸ showed evidence of increased calcium capacity of the SR, a 30% downregulation of the α_{1D} -subunit of the L-type calcium channel, and a 2-fold acceleration of inactivation rate during hibernation season in woodchuck ventricles. Thus, I_{Ca} density was found to significantly decrease and SR Ca^{2+} uptake capacity to increase in myocytes of hibernating compared with active woodchucks, which could protect the heart from calcium overload.⁴⁹ Moreover, they did find differences between active and hibernating in I_{K1} and I_{to} .²⁵

Interestingly, we previously found in the isolated papillary muscle of the Siberian GS that under different temperatures (37°C to 7°C), resting potential was mildly elevated in WH myocardium as compared to SA myocardium, but dV/dt_{max} values were not different. Based on these data and the observed improvement of threshold of excitation and accelerated conduction velocity in WH ventricles (Table 1), we suppose that upregulation of Na^{+} channels during hibernation season can play an important role in the hibernator heart protection to conduction abnormalities.

Study limitations

We showed colocalization data only for LV epicardium, in which we performed optical mapping because of technical restrictions and limits of fresh tissue samples. Moreover, our colocalization analysis was based only on immunohistochemistry, which could not show direct biochemical interaction of these proteins.

The use of di-4ANNEPS and BDM could affect the observed results because of partial ion channel blockage. However, our previous studies, in which we did not use BDM⁵ and any drugs,²⁵ showed that WH animals have the highest conduction velocity and antiarrhythmia protection compared with SA and nonhibernating rabbit and rat.

Conclusion

The WH species *Spermophilus* was protected against malignant arrhythmias such as VF because it maintained a conduction anisotropy ratio homogeneity of repolarization, and wavelength during hypothermia, and thus is protected against malignant arrhythmias such as VF. The enhanced expression and colocalization of Cx43 and N-cad during hibernation suggests that improved gap junction function is an important determinant of the maintenance of anisotropic propagation and repolarization.

Acknowledgments

The authors thank Roger Chang for looking over the article and giving grammatical suggestions.

This work was supported by the Stanley and Lucy Lopata Endowment (Dr. Efimov), the Russian Foundation for Basic Research (grant 05-04-48311), and the Russian President Foundation for Scientific School (grant SS-6211.2006.7, Dr. Rosenshtraukh).

References

1. Johansson BW. The hibernator heart—nature’s model of resistance to ventricular fibrillation. *Cardiovasc Res* 1996;31:826–832. [PubMed: 8763414]
2. Carey HV, Andrews MT, Martin SL. Mammalian hibernation: cellular and molecular responses to depressed metabolism and low temperature. *Physiol Rev* 2003;83:1153–1181. [PubMed: 14506303]
3. Andrews MT. Advances in molecular biology of hibernation in mammals. *Bioessays* 2007;29:431–440. [PubMed: 17450592]
4. Barnes BM. Freeze avoidance in a mammal: body temperatures below 0 degree C in an Arctic hibernator. *Science* 1989;244:1593–1595. [PubMed: 2740905]
5. Fedorov VV, Li L, Glukhov A, et al. Hibernator *Citellus undulatus* maintains safe cardiac conduction and is protected against tachyarrhythmias during extreme hypothermia: possible role of Cx43 and Cx45 up-regulation. *Heart Rhythm* 2005;2:966–975. [PubMed: 16171752]
6. Rozenshtraukh LV, Fedorov VV, Aliev RR, et al. Pattern of excitation in isolated heart of hibernator ground squirrel *Citellus undulatus*. *Kardiologiia* 2005;45:4–10. [PubMed: 15940184]
7. Li J, Patel VV, Kostetskii I, et al. Cardiac-specific loss of N-cadherin leads to alteration in connexins with conduction slowing and arrhythmogenesis. *Circ Res* 2005;97:474–481. [PubMed: 16100040]
8. Cheng Y, Li L, Nikolski V, et al. Shock-induced arrhythmogenesis is enhanced by 2,3-butanedione monoxime compared with cytochalasin D. *Am J Physiol Heart Circ Physiol* 2004;286:H310–H318. [PubMed: 12958029]
9. Fedorov VV, Hepmpill M, Kostecki G, et al. Low electroporation threshold, conduction block, focal activity and reentrant arrhythmia in the rabbit atria: possible mechanisms of stunning and defibrillation failure. *Heart Rhythm* 2008;5:593–604. [PubMed: 18362029]
10. Fedorov VV, Hucker WJ, Dobrzynski H, et al. Postganglionic nerve stimulation induces temporal inhibition of excitability in the rabbit sinoatrial node. *Am J Physiol* 2006;291:H612–H623.
11. Hucker WJ, McCain ML, Laughner JI, et al. Connexin 43 expression delineates two discrete pathways in the human atrioventricular junction. *Anat Rec* 2008;291:204–215.
12. Smeets JL, Alessie MA, Lammers WJ, et al. The wavelength of the cardiac impulse and reentrant arrhythmias in isolated rabbit atrium. The role of heart rate, autonomic transmitters, temperature, and potassium. *Circ Res* 1986;58:96–108. [PubMed: 3943157]
13. Severs NJ, Coppen SR, Dupont E, et al. Gap junction alterations in human cardiac disease. *Cardiovasc Res* 2004;62:368–377. [PubMed: 15094356]
14. Akar FG, Spragg DD, Tunin RS, et al. Mechanisms underlying conduction slowing and arrhythmogenesis in nonischemic dilated cardiomyopathy. *Circ Res* 2004;95:717–725. [PubMed: 15345654]
15. Wu, J.; Wu, J.; Zipes, DP.; Zipes, DP.; Jalife, J. *Cardiac Electrophysiology: From Cell to Bedside*. Saunders; Philadelphia: 2004. Mechanisms of initiation of ventricular tachyarrhythmias; p. 380-389.
16. Panfilov AV. Is heart size a factor in ventricular fibrillation? Or how close are rabbit and human hearts? *Heart Rhythm* 2006;3:862–864. [PubMed: 16818223]
17. Cao JM, Qu Z, Kim YH, et al. Spatiotemporal heterogeneity in the induction of ventricular fibrillation by rapid pacing: importance of cardiac restitution properties. *Circ Res* 1999;84:1318–1331. [PubMed: 10364570]
18. Weiss JN, Qu Z, Chen PS, et al. The dynamics of cardiac fibrillation. *Circulation* 2005;112:1232–1240. [PubMed: 16116073]
19. White JD. Cardiac arrest in hypothermia. *JAMA* 1980;244:2262. [PubMed: 7431547]
20. Dave AR, Morrison PR. Characteristics of the hibernating heart. *Am Heart J* 1955;124:367–384.
21. Duker G, Sjoquist PO, Johansson BW. Monophasic action potentials during induced hypothermia in hedgehog and guinea pig hearts. *Am J Physiol* 1987;253:H1083–H1088. [PubMed: 3688252]
22. Salama G, Kanai AJ, Huang D, et al. Hypoxia and hypothermia enhance spatial heterogeneities of repolarization in guinea pig hearts: analysis of spatial autocorrelation of optically recorded action potential durations. *J Cardiovasc Electrophysiol* 1998;9:164–183. [PubMed: 9511890]

23. Saitongdee P, Milner P, Becker DL, et al. Increased connexin43 gap junction protein in hamster cardiomyocytes during cold acclimatization and hibernation. *Cardiovasc Res* 2000;47:108–115. [PubMed: 10869536]
24. Anufriev, AI.; Akhremenko, AK. Dependence of frequency of *Citellus undulatus* arousal on ambient temperature. In: Kolaeva, S.; Popova, M.; Solomonov, N.; Wang, L., editors. *Mechanisms of Natural Hypometabolic States*. Vol. 8. PSC RAS Puschino; Moscow: 1992. p. 34-38.
25. Glukhov AV, Egorov Y, Fedorov VV, et al. The effect of hypothermia on the wavelength and vulnerability to ventricular arrhythmias in mammals. *Russ Fiziol Zh Im IM Sechenova* 2007;93:289–299. [PubMed: 17598472]
26. Spach MS, Miller WT 3, Geselowitz DB, et al. The discontinuous nature of propagation in normal canine cardiac muscle. Evidence for recurrent discontinuities of intracellular resistance that affect the membrane currents. *Circ Res* 1981;48:39–54. [PubMed: 7438345]
27. Spach MS, Heidlage JF, Dolber PC, et al. Mechanism of origin of conduction disturbances in aging human atrial bundles: experimental and model study. *Heart Rhythm* 2007;4:175–185. [PubMed: 17275753]
28. Duker GD, Olsson SO, Hecht NH, et al. Ventricular fibrillation in hibernators and nonhibernators. *Cryobiology* 1983;20:407–420. [PubMed: 6617230]
29. Kirchhof PF, Fabritz CL, Franz MR. Postrepolarization refractoriness versus conduction slowing caused by class I antiarrhythmic drugs: antiarrhythmic and proarrhythmic effects. *Circulation* 1998;97:2567–2574. [PubMed: 9657478]
30. Spach MS, Heidlage JF, Dolber PC, et al. Electrophysiological effects of remodeling cardiac gap junctions and cell size: experimental and model studies of normal cardiac growth. *Circ Res* 2000;86:302–311. [PubMed: 10679482]
31. Shaw RM, Rudy Y. Ionic mechanisms of propagation in cardiac tissue. Roles of the sodium and L-type calcium currents during reduced excitability and decreased gap junction coupling. *Circ Res* 1997;81:727–741. [PubMed: 9351447]
32. Poelzing S, Akar FG, Baron E, et al. Heterogeneous connexin43 expression produces electrophysiological heterogeneities across ventricular wall. *Am J Physiol Heart Circ Physiol* 2004;286:H2001–H2009. [PubMed: 14704225]
33. Rohr S, Kucera JP, Fast VG, et al. Paradoxical improvement of impulse conduction in cardiac tissue by partial cellular uncoupling. *Science* 1997;275:841–844. [PubMed: 9012353]
34. Gutstein DE, Morley GE, Tamaddon H, et al. Conduction slowing and sudden arrhythmic death in mice with cardiac-restricted inactivation of connexin43. *Circ Res* 2001;88:333–339. [PubMed: 11179202]
35. Danik SB, Liu F, Zhang J, et al. Modulation of cardiac gap junction expression and arrhythmic susceptibility. *Circ Res* 2004;95:1035–1041. [PubMed: 15499029]
36. Bukauskas FF, Weingart R. Temperature dependence of gap junction properties in neonatal rat heart cells. *Pflugers Arch* 1993;423:133–139. [PubMed: 7683787]
37. Kojodjojo P, Kanagaratnam P, Segal OR, et al. The effects of carbenoxolone on human myocardial conduction: a tool to investigate the role of gap junctional uncoupling in human arrhythmogenesis. *J Am Coll Cardiol* 2006;48:1242–1249. [PubMed: 16979013]
38. Eloff BC, Gilat E, Wan X, et al. Pharmacological modulation of cardiac gap junctions to enhance cardiac conduction: evidence supporting a novel target for antiarrhythmic therapy. *Circulation* 2003;108:3157–3163. [PubMed: 14656916]
39. Xing D, Kjolbye AL, Nielsen MS, et al. ZP123 increases gap junctional conductance and prevents reentrant ventricular tachycardia during myocardial ischemia in open chest dogs. *J Cardiovasc Electrophysiol* 2003;14:510–520. [PubMed: 12776869]
40. Gutstein DE, Liu FY, Meyers MB, et al. The organization of adherens junctions and desmosomes at the cardiac intercalated disc is independent of gap junctions. *J Cell Sci* 2003;116:875–885. [PubMed: 12571285]
41. Shaw RM, Fay AJ, Puthenveedu MA, et al. Microtubule plus-end-tracking proteins target gap junctions directly from the cell interior to adherens junctions. *Cell* 2007;128:547–560. [PubMed: 17289573]

42. Ferreira-Cornwell MC, Luo Y, Narula N, et al. Remodeling the intercalated disc leads to cardiomyopathy in mice misexpressing cadherins in the heart. *J Cell Sci* 2002;115:1623–1634. [PubMed: 11950881]
43. Wei CJ, Francis R, Xu X, et al. Connexin43 associated with an N-cadherin-containing multiprotein complex is required for gap junction formation in NIH3T3 cells. *J Biol Chem* 2005;280:19925–19936. [PubMed: 15741167]
44. Hertig CM, Eppenberger-Eberhardt M, Koch S, et al. N-cadherin in adult rat cardiomyocytes in culture. I. Functional role of N-cadherin and impairment of cell-cell contact by a truncated N-cadherin mutant. *J Cell Sci* 1996;109:1–10. [PubMed: 8834785]
45. Stein M, Noorman M, van Veen TA, et al. Dominant arrhythmia vulnerability of the right ventricle in senescent mice. *Heart Rhythm* 2008;5:438–448. [PubMed: 18313604]
46. Liu B, Zhao MJ, Chao I. Effect of cold on transmembrane potentials in cardiac cells of the hedgehog. *J Therm Biol* 1987;12:77–80.
47. Liu B, Arlock P, Wohlfart B, et al. Temperature effects on the Na and Ca currents in rat and hedgehog ventricular muscle. *Cryobiology* 1991;28:96–104. [PubMed: 2015764]
48. Yatani A, Kim SJ, Kudej RK, et al. Insights into cardioprotection obtained from study of cellular Ca²⁺ handling in myocardium of true hibernating mammals. *Am J Physiol Heart Circ Physiol* 2004;286:H2219–H2228. [PubMed: 14962828]
49. Wang SQ, Lakatta EG, Cheng H, et al. Adaptive mechanisms of intracellular calcium homeostasis in mammalian hibernators. *J Exp Biol* 2002;205:2957–2962. [PubMed: 12200399]

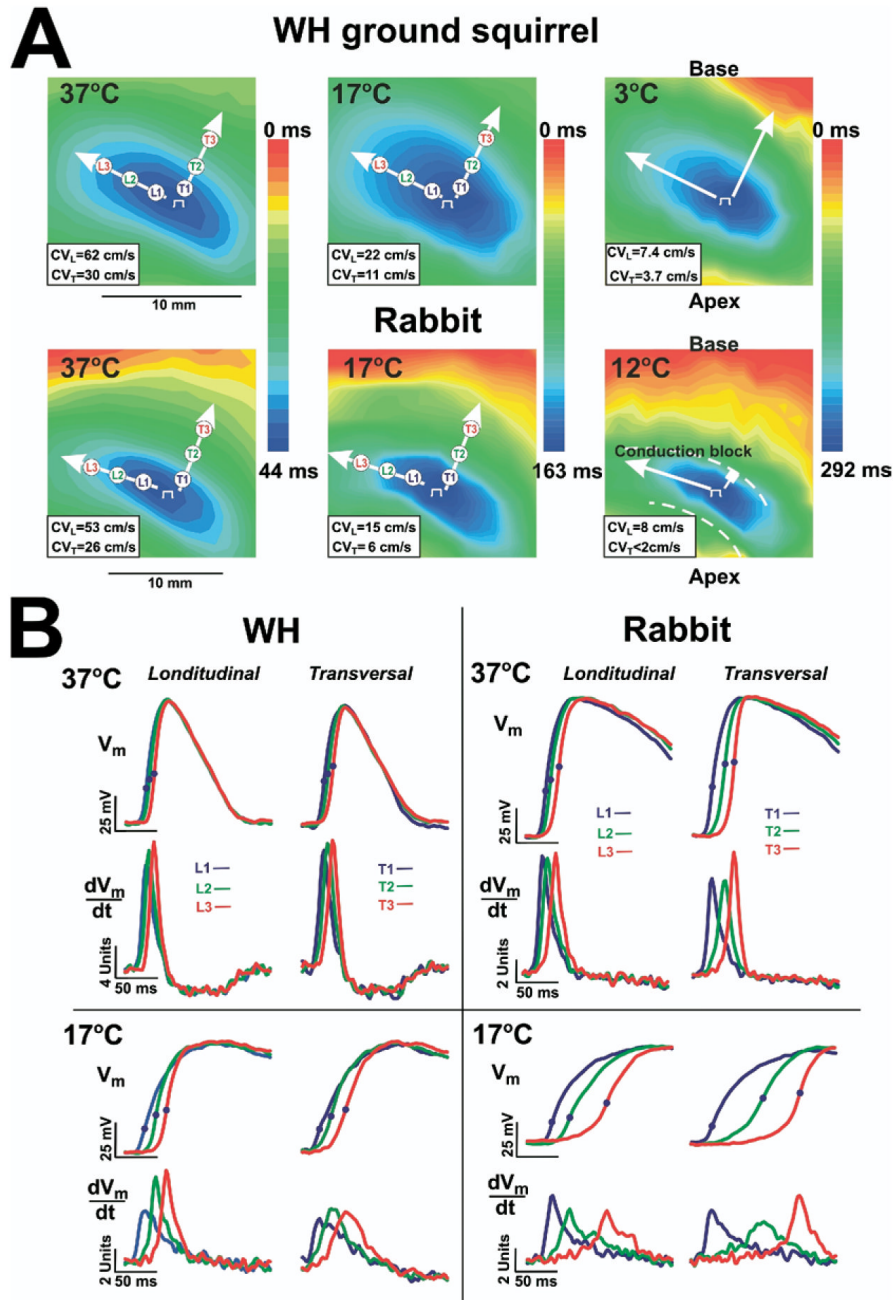


Figure 1. The effect of hypothermia on the left ventricular activation pattern. **A:** Optical maps during epicardial pacing of the winter-hibernating (WH) ground squirrel and rabbit heart shown at various temperatures during pacing (400 ms at 37°C, 1,000 ms at 17°C, 2,000 ms at 12°C, and 4,000 at 3°C, respectively). Epicardial pacing at the center of the left ventricle produced an ellipsoidal spread of propagation with fast conduction parallel to the fiber axis (longitudinal conduction) and slow conduction perpendicular to the fiber axis (transverse conduction). Arrows show the directions of conduction velocity measurements longitudinal (CV_L) and transversal (CV_T). The values of corresponding CVs are presented at the right bottom corner of each map. **B:** Superimposed upstrokes of optical APs and their derivatives corresponding

to recording sites in longitudinal direction L1, L2, and L3 and transversal T1, T2, and T3 in maps in panel A. Optical APs were normalized to range from -77 to +12 mV (WH) and from -85 to +15 mV (rabbit) 37 °C, range from -65 to 17 mV (WH) and -61 to +5 mV (rabbit) at 17°C using previously published microelectrode data.⁵

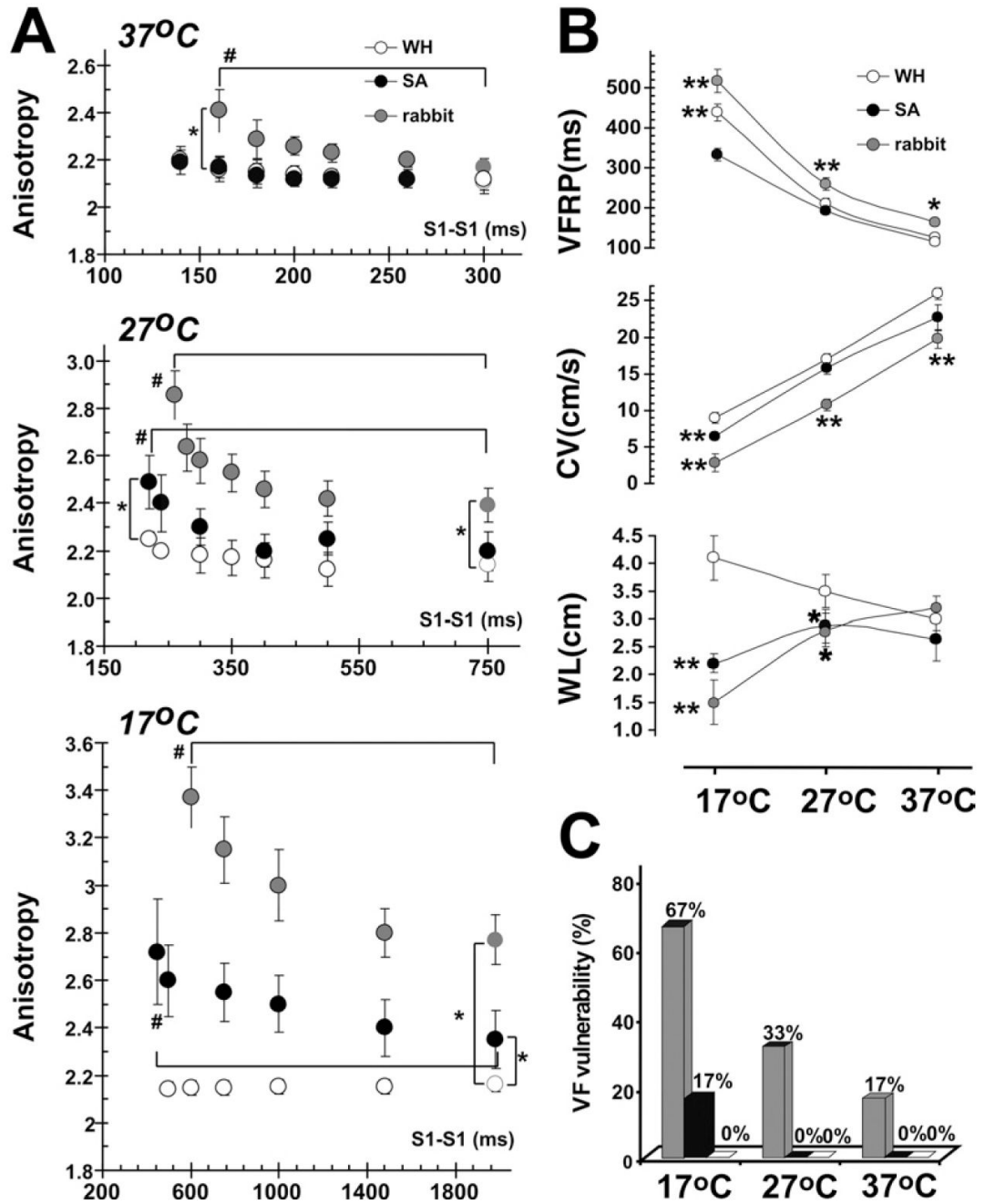


Figure 2. The influence of hypothermia on the main electrophysiological parameters and ventricular fibrillation (VF) vulnerability. **A:** Ventricular functional refractory period (VFRP), the minimal conduction velocity (CV) and the wavelength during maximum pacing rate (WL) in rabbit and ground squirrel hearts. Data summarizes summer-active (SA) and winter-hibernating (WH) ground squirrels (black and white circles) and rabbits (red circles). **B:** Conduction anisotropy versus pacing cycle length at different temperatures in rabbit and ground squirrel hearts. The anisotropy index was calculated as the ratio of longitudinal and transversal components of conduction velocity. * $P < .05$ versus WH ground squirrel. # $P < .05$

versus 37 °C. **C:** Effect of hypothermia on incidence of pacing-induced ventricular fibrillation (VF) in rabbit and ground squirrel hearts.

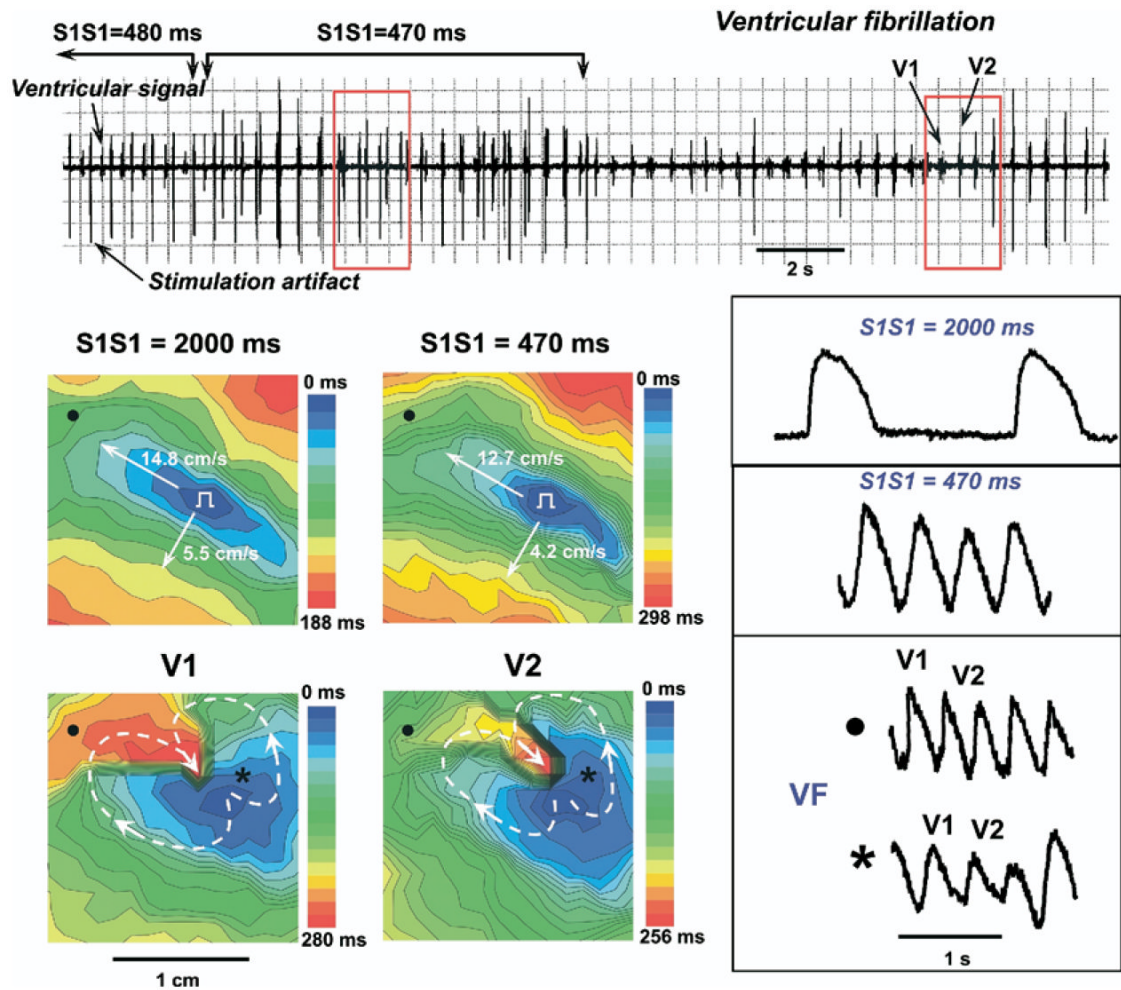


Figure 3. Induction of ventricular fibrillation in rabbit heart during fast pacing at 17°C. On the ventricular bipolar electrogram at the top, a recording of ventricular stimulation with progressively shortening pacing interval are presented. Red frames indicate the mapped space. V1 and V2 are mapped VF waves. The gradual shortening of the pacing interval from 2,000 ms to 470 ms (top maps) leads to increasing the conduction anisotropy because of the depression of conduction velocity along the transverse direction. Representative traces of optical transmembrane action potentials recorded from right (●) and left (*) ventricle areas are presented near activation maps.

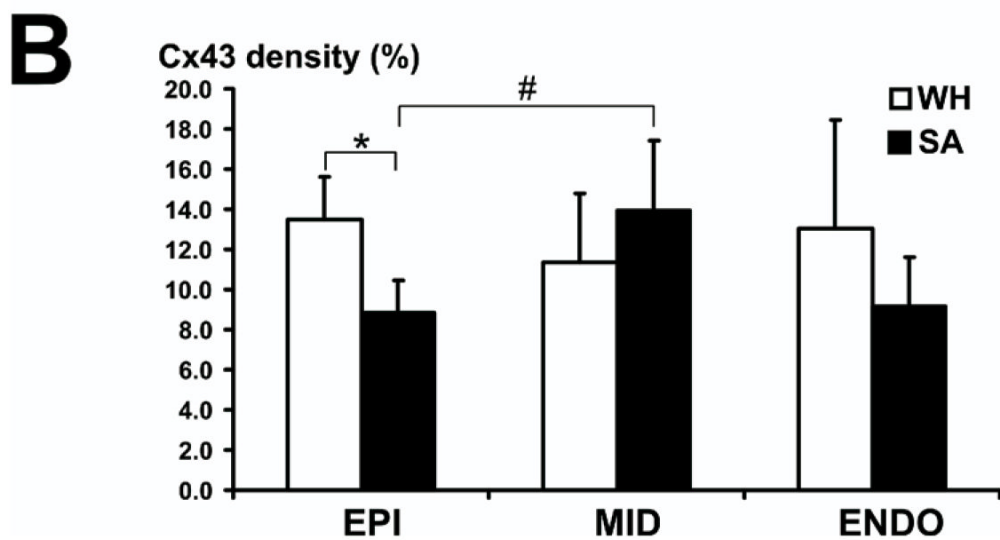
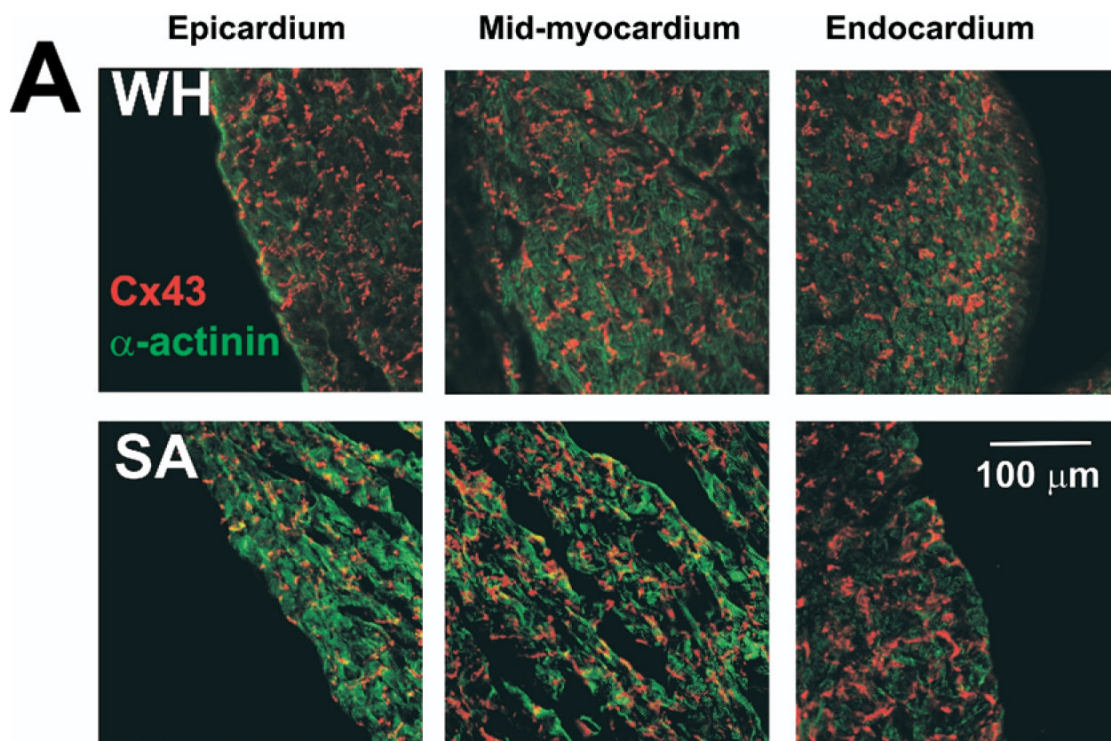


Figure 4. Transmurally expression of connexin 43. **A:** Sample confocal images from a winter-hibernating (WH) and summer-active (SA) heart taken from endocardial, midcardial, and epicardial locations. **B:** Average connexin 43 densities at each tissue location. We analyzed 5 sister sections from epicardial and midcardial and 4 sections from endocardial for each animal WH (n = 3) and SA (n = 3). * $P < .05$ versus WH ground squirrel. # $P < .05$ versus epicardium.

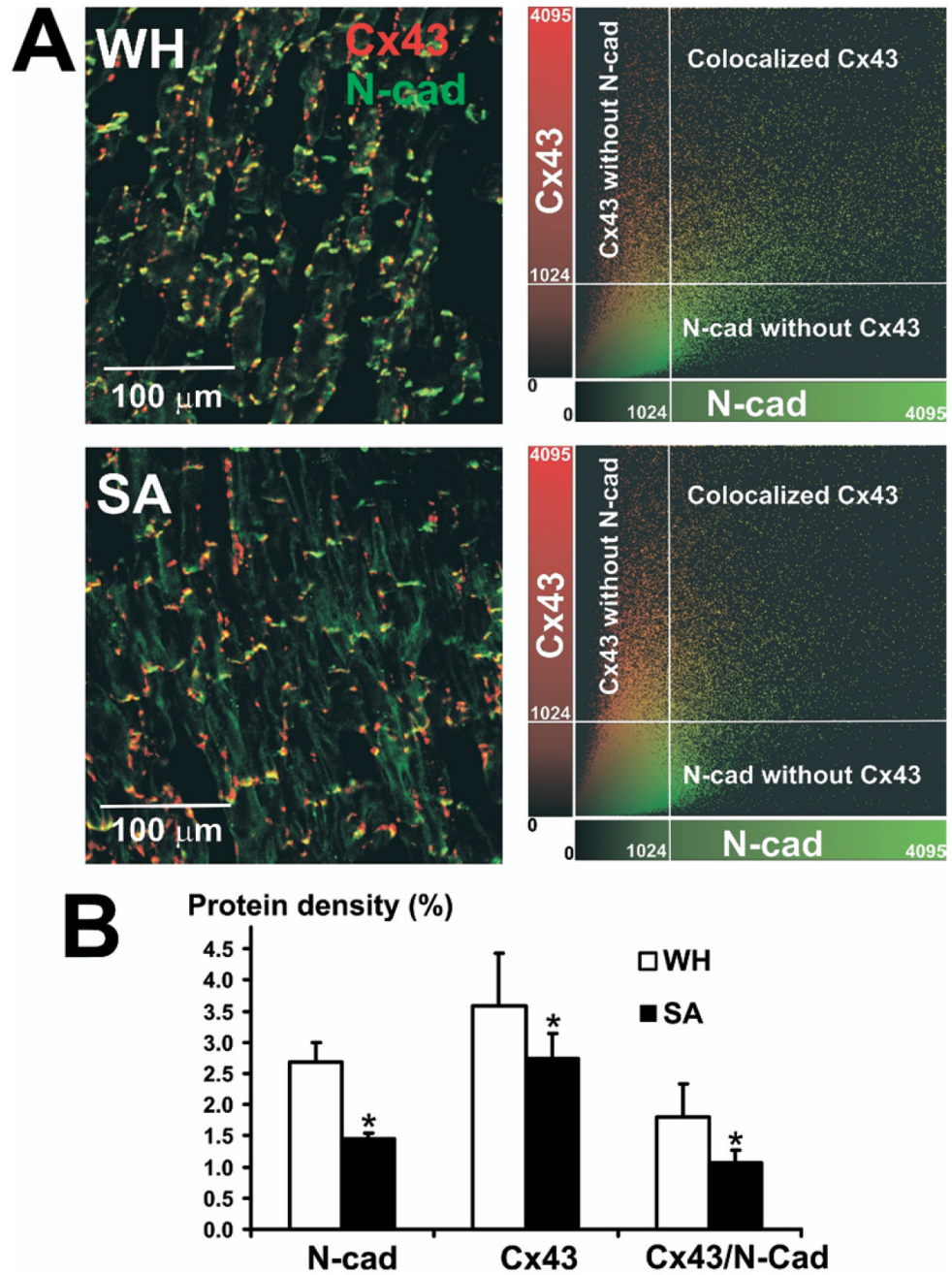


Figure 5. Expression of connexin 43 (Cx43) and N-cadherins (N-cad), and their colocalization in epicardium of winter-hibernating (WH) and summer-active (SA) ground squirrels. **A, Left:** Immunohistochemical images of Cx43 (red) and N-cad (green) staining in the WH and SA left ventricular epicardium. **A, Right:** Colocalization of Cx43 and N-cad, showing that voxels of high Cx43 intensity also have a high N-cad signal in both WH and SA. However, the amount of colocalized Cx43 in WH is higher than in SA. Intensity level of 1,024 units was used as a threshold. **B:** Summary density of N-cad, total Cx43, and colocalized Cx43 with N-cad. We analyzed 4 sister sections from epicardium for each animal WH (n = 4) and SA (n = 4). * $P < .05$ versus WH ground squirrel. See text for details.

Table 1
Main electrophysiological parameters at basic cycle length vs. temperature for WH and SA ground squirrel and rabbit hearts

Parameters	Species CL	37°C 300 ms	27°C 750 ms	17°C 2000 ms	7°C 2000 ms	3°C 5000 ms
Threshold (mA)	Rabbit	1.0 ± 0.1	1.4 ± 0.1 ^{*,#}	2.2 ± 0.2 ^{**,#}	—	—
	SA	0.9 ± 0.1	1.3 ± 0.1 ^{*,#}	1.4 ± 0.1 ^{*,#}	1.7 ± 0.2 ^{*,#}	2.3 ± 0.3 ^{*,#}
	WH	0.8 ± 0.1	0.7 ± 0.1	0.9 ± 0.1	1.1 ± 0.1	1.5 ± 0.2 [#]
CV _L (cm/s)	Rabbit	55.7 ± 1.5 ^{**}	37.8 ± 2.0 ^{**}	13.8 ± 1.0 ^{**}	—	—
	SA	60.8 ± 2.2 [*]	46.5 ± 1.2	23.5 ± 1.8	8.9 ± 0.4	5.4 ± 0.3
	WH	67.0 ± 0.7	48.0 ± 2.7	25.4 ± 1.7	9.3 ± 0.4	6.9 ± 0.4
CV _T (cm/s)	Rabbit	25.7 ± 1.0 ^{**}	15.8 ± 0.8 ^{**}	5.0 ± 0.4 ^{**}	—	—
	SA	28.8 ± 1.7	21.3 ± 0.9	10.0 ± 0.4	3.9 ± 0.2	2.5 ± 0.2 [*]
	WH	31.8 ± 0.8	22.6 ± 1.2	11.8 ± 0.9	4.4 ± 0.2	3.1 ± 0.2
Anisotropy	Rabbit	2.17 ± 0.04	2.39 ± 0.03 ^{**}	2.77 ± 0.04 ^{**}	—	—
	SA	2.12 ± 0.06	2.20 ± 0.08	2.35 ± 0.12 [*]	2.41 ± 0.11 [*]	2.49 ± 0.12 [*]
	WH	2.11 ± 0.05	2.12 ± 0.02	2.16 ± 0.04	2.20 ± 0.07	2.26 ± 0.09
APD (ms)	Rabbit	179 ± 10 ^{**}	358 ± 29 ^{**}	613 ± 6 ^{**}	—	—
	SA	124 ± 6 ^{**}	239 ± 8 ^{**}	495 ± 32 [*]	703 ± 22 ^{**}	833 ± 30 [*]
	WH	101 ± 3	201 ± 6	397 ± 22	604 ± 11	728 ± 31
SD-APD (ms)	Rabbit	9 ± 2	18 ± 2 [*]	42 ± 4 ^{**}	—	—
	SA	7 ± 1	10 ± 2	30 ± 4 [*]	53 ± 7 [*]	81 ± 13 [*]
	WH	5 ± 1	8 ± 2	18 ± 3	36 ± 7	51 ± 5
Dmax (ms)	Rabbit	38 ± 8 [*]	59 ± 12 [*]	144 ± 28 ^{**}	—	—
	SA	29 ± 3	37 ± 5	105 ± 17 [*]	180 ± 14 [*]	274 ± 29 [*]
	WH	21 ± 3	35 ± 6	76 ± 9	130 ± 6	179 ± 14

Rabbit (n = 6); SA = summer active (n = 8); WH = winter hibernating (n = 8); Group data are represented as mean ± SEM.

* - $p < 0.05$

** - $p < 0.01$ vs WH

- $p < 0.05$ vs 37C for the same species.

Table 2
Main electrophysiological parameters at VFRP vs. temperature for WH and SA ground squirrel and rabbit hearts

Parameters	Species	37°C	27°C	17°C
VFRP (ms)	Rabbit	162 ± 2 ^{**}	257 ± 16 [*]	515 ± 29 ^{**}
	SA	114 ± 4	190 ± 8	331 ± 15
	WH	124 ± 6	209 ± 14	436 ± 22
CV _L (cm/s)	Rabbit	47.5 ± 2.2 [*]	29.2 ± 2.3 [*]	9.4 ± 0.7 ^{**}
	SA	50.8 ± 3.0 [*]	38.5 ± 2.1	17.8 ± 1.8
	WH	56 ± 0.7	37.6 ± 1.5	19.0 ± 1.4
CV _T (cm/s)	Rabbit	19.8 ± 1.3 [*]	10.8 ± 0.8 ^{**}	2.8 ± 0.3 ^{**}
	SA	23.3 ± 1.8	15.8 ± 0.8	6.5 ± 0.3 [*]
	WH	25.4 ± 0.6	16.6 ± 0.7	8.9 ± 0.7
WL _L (cm/s)	Rabbit	7.7 ± 0.3 [*]	7.5 ± 0.8	4.9 ± 0.5 ^{**#}
	SA	5.6 ± 0.7	7.4 ± 0.6 [#]	6.1 ± 0.6 [*]
	WH	6.5 ± 0.3	8.0 ± 0.8 [#]	8.7 ± 0.9 [#]
WL _T (cm/s)	Rabbit	3.2 ± 0.2	2.8 ± 0.3 [*]	1.5 ± 0.2 ^{**#}
	SA	2.6 ± 0.4	2.9 ± 0.3 [*]	2.2 ± 0.1 ^{**#}
	WH	3.0 ± 0.2	3.5 ± 0.3	4.1 ± 0.4 [#]
Anisotropy	Rabbit	2.41 ± 0.06 [*]	2.69 ± 0.09 ^{**#}	3.37 ± 0.13 ^{**#}
	SA	2.19 ± 0.06	2.49 ± 0.11 [#]	2.72 ± 0.22 ^{**#}
	WH	2.21 ± 0.03	2.26 ± 0.04	2.14 ± 0.03

Rabbit (n = 6); SA = summer active (n = 8); WH = winter hibernating (n = 7); Group data are represented as mean ± SEM.

* - $p < 0.05$

** - $p < 0.01$ vs WH

- $p < 0.05$ vs 37C for the same species.